

## Separating spin and charge transport in single-wall carbon nanotubes

N. Tombros, S. J. van der Molen, and B. J. van Wees

*Physics of Nanodevices, Materials Science Centre, Rijksuniversiteit Groningen, Nijenborgh 4, 9747 AG Groningen, The Netherlands*

(Received 10 April 2006; published 9 June 2006)

We demonstrate spin injection and detection in single wall carbon nanotubes using a four-terminal nonlocal geometry. This measurement geometry completely separates the charge and spin circuits. Hence all spurious magnetoresistance effects are eliminated and the measured signal is due to spin accumulation only. Combining our results with a theoretical model, we deduce a spin polarization at the contacts  $\alpha_F$  of approximately 25%. We show that the magnetoresistance changes measured in the conventional two-terminal geometry are only partly due to spin accumulation.

DOI: [10.1103/PhysRevB.73.233403](https://doi.org/10.1103/PhysRevB.73.233403)

PACS number(s): 72.25.-b, 81.07.De, 85.75.-d

Single wall carbon nanotubes (SWNT's) behave as almost ideal one-dimensional conductors, having a small diameter (typically a nanometer), on the one hand, and a large scattering mean free path, on the other.<sup>1</sup> Additionally, it is expected that electronic spin flip scattering in SWNT's is weak. This makes them excellent candidates for spintronic devices, in which the nanotubes are contacted by ferromagnetic leads. Despite the promise that the combination of nanotubes and spintronics holds, there have been no experiments so far that unequivocally demonstrate spin accumulation in carbon nanotubes. In fact, all experiments performed since the pioneering work of Tsukagoshi *et al.*<sup>2</sup> have made use of the conventional two-terminal spin valve geometry.<sup>3-12</sup> Unfortunately, in this geometry, it is difficult to separate spin transport from other effects, such as Hall effects, anisotropic magnetoresistance,<sup>13,14</sup> interference effects,<sup>15</sup> tunneling anisotropic magnetoresistancelike effects,<sup>11,16</sup> and magneto-Coulomb effects.<sup>17,18</sup> These may obscure and even mimic the spin accumulation signal. With a four-terminal nonlocal spin valve geometry,<sup>13,19,20</sup> one is able to completely separate the spin current path from the charge current path. Hence, the signal measured is due to spin transport only. With this technique we unambiguously demonstrate spin accumulation in single wall carbon nanotubes.

To determine spin accumulation in the nonlocal geometry [see Fig. 1(c)], one needs to contact a metallic SWNT with four electrodes. At least two of these should be ferromagnetic. They act as spin injector and spin detector, respectively. For practical reasons, we make use of four ferromagnetic contacts. These electrodes are narrow, but of different widths to assure different switching fields  $B_C$  ( $B_C$  decreases with increasing width).<sup>13,20</sup> Single wall carbon nanotubes (>90% SWNT's) (Ref. 21) are dispersed in HPLC grade chlorobenzene. We use the alternating current dielectrophoresis technique<sup>22</sup> to deposit the SWNT's at a predefined area on the substrate. An atomic force microscope (AFM) in tapping mode is used to locate and characterize the SWNT's on the SiO<sub>2</sub> surface. Conventional electron beam lithography and *e*-beam evaporation (45 nm of Co at  $4.0 \times 10^{-7}$  mbar) are used to define the contacts. To avoid damaging the nanotube, no additional cleaning is done before deposition.

Although we regularly obtain low contact resistances ( $\sim k\Omega$ ), the preparation of the device is not trivial, as all the contacts have to be low ohmic. It is also crucial that electron

and spin transport can occur through the entire nanotube, including the regions underneath the Co contacts. Out of 15 devices, we obtained one device that fulfilled these requirements.<sup>23</sup> In Fig. 1 it is depicted. The two outermost electrodes  $F_1$  and  $F_4$  have a width of 200 nm. The two central electrodes  $F_2$  and  $F_3$  have a width of 70 and 90 nm, respectively. The nanotube itself has a diameter of

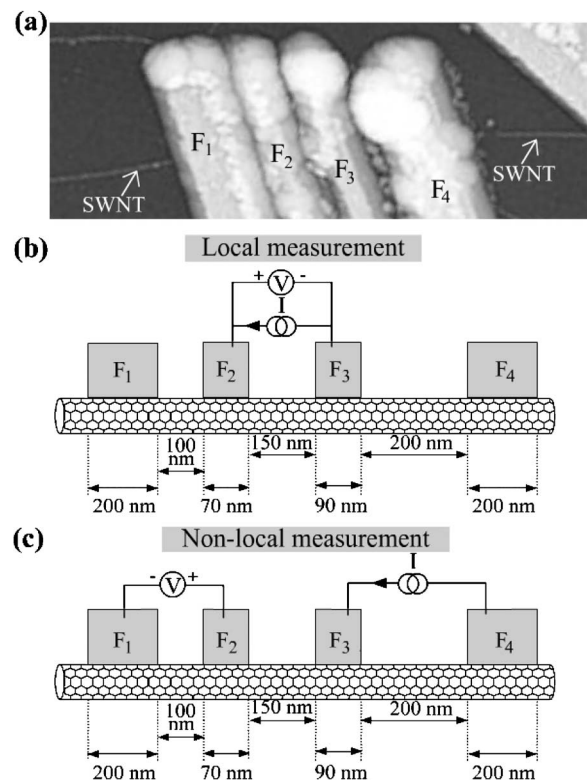


FIG. 1. A single wall carbon nanotube ( $d=3.4 \pm 0.4$  nm; possibly it is a bundle containing a few nanotubes) contacted by four ferromagnetic (cobalt) electrodes. (a) An AFM picture of the device. Note that imperfect lift off resulted in some PMMA residue on top of the cobalt electrodes, this partially obscures the well defined Co electrodes underneath (Ref. 31). (b) Geometry of a conventional spin valve (or “local”) measurement, in which contacts  $F_2$  and  $F_3$  are used both to inject current and to measure voltage. (c) The “nonlocal” geometry. In this case the voltage circuit ( $F_1$ -SWNT- $F_2$ ) is completely separated from the current circuit ( $F_3$ -SWNT- $F_4$ ).

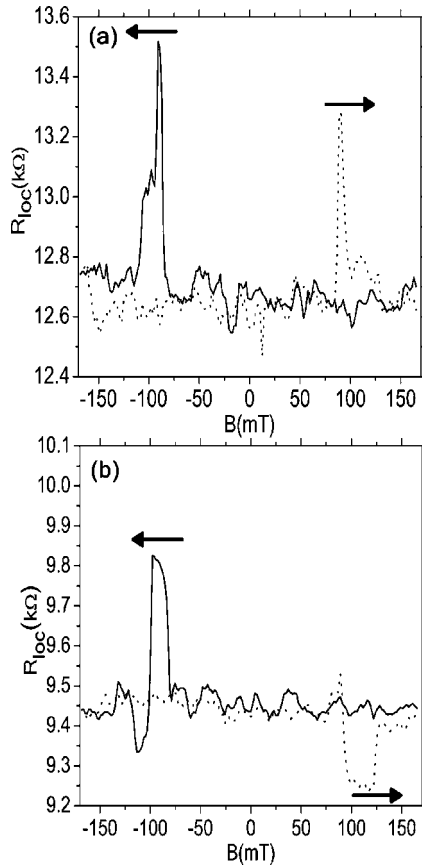


FIG. 2. Two-terminal spin valve measurements ( $F_2$ -SWNT- $F_3$ ,  $I=10$  nA) at 4.2 K [see Fig. 1(b)]. (a) Upon sweeping the  $B$  field, the “local” resistance increases when  $|B|$  reaches  $\approx 80$  mT. It falls back to its original value when  $|B|$  increases further.  $\Delta R/R$  has a maximum value of  $\approx 6\%$ . We observe significant substructure on top of the resistance peaks. (b) A similar measurement on the same sample (also at 4.2 K, but with a thermal cycling step in between). The magnetoresistance trace is completely different from the traces in a) and shows both positive and negative values for  $\Delta R/R$ .

$3.4 \pm 0.4$  nm (we cannot exclude that it is a bundle containing a few SWNT’s). To measure the transport properties of the nanotube, we make use of a standard ac lock-in technique (maximum current, 60 nA). At 4.2 K, we find two-terminal resistances of 28, 12.4, 15, 44.3, 22.8, and 52.6 k $\Omega$  between contacts  $F_1$ - $F_2$ ,  $F_2$ - $F_3$ ,  $F_3$ - $F_4$ ,  $F_1$ - $F_3$ ,  $F_2$ - $F_4$ , and  $F_1$ - $F_4$ , respectively. A four-terminal measurement (current from  $F_1$ - $F_4$ ; voltage between  $F_2$  and  $F_3$ ) gives a resistance of 10.3 k $\Omega$ , equivalent to a conductance of  $2.5e^2/h$ . Since these values are quite close to  $4e^2/h$ , we are probing at least one metallic (or degenerate semiconductor) SWNT. From the values above, we deduce the contact resistances between the nanotube and electrodes  $F_2$  and  $F_3$ . Comparing the four-terminal resistance with the two-terminal measurement ( $F_2$ - $F_3$ ), we get values around a k $\Omega$ .

Next, we investigate the two-terminal “spin valve” effect between contacts  $F_2$  and  $F_3$  [see Fig. 1(b)]. For this, we continuously sweep the magnetic field back and forth between  $-165$  and  $165$  mT (at 4.2 K). Two characteristic traces are shown in Fig. 2(a). The behavior found is generally described as follows. Let us start at  $B=165$  mT, where  $F_2$  and

$F_3$  are both magnetized parallel to the external field. When the field is subsequently swept to negative values,  $F_3$  (being the widest) will flip magnetization as soon as the external field equals its switching field. Consequently, the magnetizations of  $F_2$  and  $F_3$  are now antiparallel, leading to a resistance increase. When the  $B$  field gets more negative, also  $F_2$  switches, so that the magnetizations of both are parallel again. This leads to a resistance decrease, back to the original value. A magnetoresistance change of approximately 6% is observed in Fig. 2(a). This is a considerable effect, comparable to the values reported in Ref. 2 ( $\leq 9\%$ ).

Although it appears that Fig. 2(a) can be explained as a result of spin transport only, we argue that this is not the case. Figure 2(b) shows an experiment performed on the same sample in the exact same measurement geometry, at 4.2 K. [There is a thermal cycling step in between Figs. 2(a) and 2(b)]. A completely different behavior is observed. A predominantly negative, instead of positive, magnetoresistance signal is now seen at positive  $B$  fields.<sup>24</sup> Similar negative magnetoresistances have been observed in multiwall<sup>5-7</sup> and single wall<sup>12</sup> carbon nanotubes. It is nontrivial to explain these effects from spin transport only (they would require a sign change in the polarization at only one of the electrodes).<sup>25</sup> Another curiosity, often observed in nanotubes (although not by us), is the fact that the magnetoresistance increases before the external field has even changed sign.<sup>2,5,14</sup> The problem in the interpretation lies in the fact that many other phenomena, not related to spin, influence the magnetoresistance.<sup>13-15,17,18</sup> Without extra knowledge these are inseparable from spin accumulation in a two-terminal experiment.

Fortunately, spin accumulation can be isolated from spurious effects by adopting the nonlocal measurement geometry [see Fig. 1(c)].<sup>13,19,20</sup> In such experiments, the charge current path is completely separated from the *spin* current path. In our case, this is done by attaching the current probes to  $F_3$  ( $I^+$ ) and  $F_4$  ( $I^-$ ) and the voltage probes to  $F_2$  ( $V^+$ ) and  $F_1$  ( $V^-$ ), thus measuring the “nonlocal” magnetoresistance  $R_{\text{nonloc}} \equiv (V^+ - V^-)/I$ . In Figs. 3(a) and 3(b), we display two sets of measurements. A clear and clean switching behavior is seen for all traces. These results are similar to those obtained by Jedema *et al.* for Al wires.<sup>20</sup> Characteristic is the change of sign from positive (+15  $\Omega$ ) to negative ( $-5$   $\Omega$ ) resistance values. This sign change can only happen if the voltage probe  $F_2$  (“detector”) measures spin accumulation in the SWNT system. In fact, when the voltage probe  $F_2$  is parallel to the spin “injector”  $F_3$ , it probes the (positive) electrochemical potential of the majority spin species (giving positive nonlocal resistance). However, when its magnetization is antiparallel to that of  $F_3$ , it probes the (negative) chemical potential of the minority spins. The change of sign thus assures us that we are measuring spin accumulation (ruling out more complicated current paths such as observed in multiwall nanotubes).<sup>26</sup> We note that an important feature in Fig. 3 is the reduction of the noise ( $\approx 3$   $\Omega$ ), as compared to Fig. 2 ( $\approx 50$   $\Omega$ ). This illustrates the insensitivity of nonlocal measurements with respect to fluctuations in the overall resistance. Figure 3(d) shows a nonlocal measurement after a thermal annealing step to room temperature. Also in this case

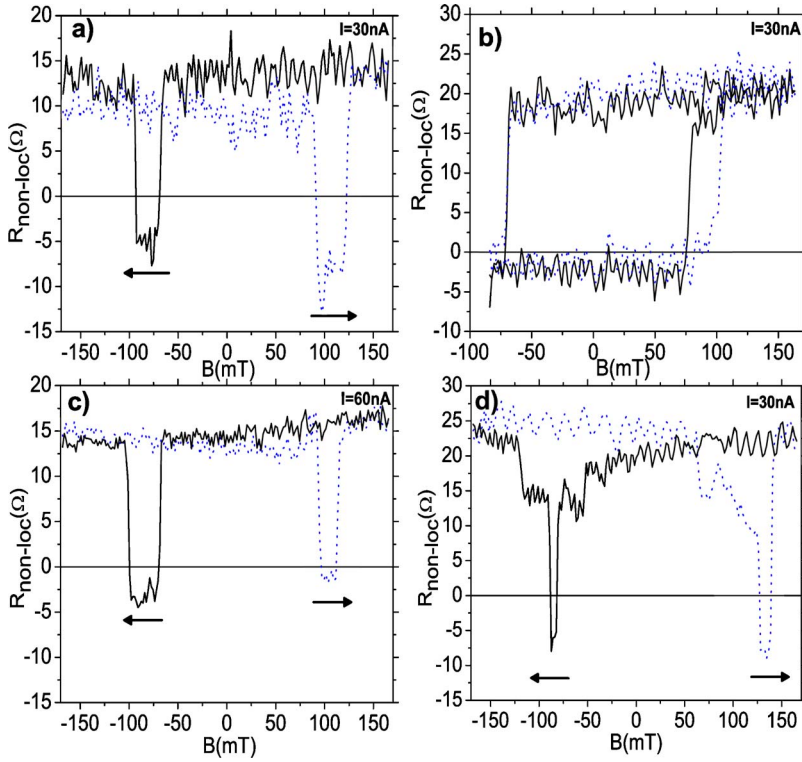


FIG. 3. (Color online) Nonlocal measurements at  $T=4.2$  K. The current path (from  $F_3$  to  $F_4$ ) is separated from the voltage probes [ $F_2$  to  $F_1$ , see Fig. 1(c)]. The observed resistance switching is due to spin accumulation and spin transport in the single wall carbon nanotube. (a) Full magnetic field scan with an ac current of 30 nA.  $R_{\text{nonloc}}$  is negative when the spin injector  $F_3$  is magnetized antiparallel to the spin detector  $F_2$ . In this situation the detector measures mainly the negative chemical potential of the minority spin species. (b) The memory effect ( $I=30$  nA), in which only the magnetization of  $F_3$  is switched. (c) Similar measurement to (a), but now with an ac current of 60 nA, resulting in a reduction of the resistance noise level. (d) Nonlocal measurement similar to (a), with  $I=30$  nA. Between (a)–(c) and (d), respectively, the sample was annealed to room temperature.

we observe a clear change of sign.<sup>27</sup> As an extra confirmation, we measure the so-called “memory effect” in the nonlocal geometry [Fig. 3(c)]. This hysteresis effect is generated by allowing only one of the two central electrodes to switch. We start at  $B=165$  mT for which the magnetizations of  $F_2$  and  $F_3$  are parallel and the nonlocal resistance is positive. Subsequently, we decrease the magnitude of the applied magnetic field to negative values until  $F_3$  switches at  $\approx -70$  mT. Now  $F_2$  and  $F_3$  are antiparallel and  $R_{\text{nonloc}}$  becomes negative. Next, we sweep to positive fields again ( $F_2$ ,  $F_3$  are still antiparallel) until at  $\approx 70$  mT electrode  $F_3$  switches back. Thus we have returned to the original situation. This demonstrates that the magnetization of one individual electrode determines the sign of the measurement.

Comparing Fig. 2 with Fig. 3, an interesting observation can be made. Whereas in the conventional spin valve measurement a magnetoresistance change  $\Delta R_{\text{loc}} \approx 700 \Omega$  is found, the “nonlocal” experiment yields  $\Delta R_{\text{nonloc}} = 20 \Omega$ , i.e., only 3% of the “local” value. This raises the question if the large spin valve effect in Fig. 2 originates from spin accumulation or from spurious phenomena. To answer this, we model the spin imbalance within the nanotube using a resistor network (see Fig. 4). We assume the spin flip length,  $\lambda_{sf}$  to exceed all sample dimensions. The (spin-independent) nanotube resistance between contacts  $i$  and  $i+1$  is denoted by  $R_{i,i+1}$ . Here we use two models. In model A, we assume a diffusive nanotube such that  $R_{i,i+1} \neq 0$ . In model B, we assume  $R_{i,i+1} = 0$  (ballistic nanotube, see Ref. 28). The contact resistance at each electrode is split in two spin-dependent terms:  $r_{i,\uparrow}$  and  $r_{i,\downarrow}$  (where  $\eta = \uparrow, \downarrow$  denotes spin direction). Both are calculated, assuming a contact conductivity  $\sigma_{\uparrow(\downarrow)} = \sigma_0(1 \pm \alpha_F)/2$ , where  $0 < \alpha_F < 1$  denotes the spin polarization. We have measured all possible combina-

tions of two-, three-, and four-probe resistances in the SWNT device. From this we can determine the contact resistances between the nanotube and contacts  $F_2$  and  $F_3$ . The contact resistances between the nanotube and contacts  $F_1$  and  $F_4$  cannot be precisely determined and are assumed equal to those of  $F_2$  and  $F_3$ .<sup>29</sup> From the model, the contact resistances, and the nonlocal traces, we obtain a spin polarization  $\alpha_F \approx 0.25$ .<sup>27</sup> We note that this is only a factor of two smaller than what is ideally attainable. This indicates that the assumption of  $\lambda_{sf}$  being large in a carbon nanotube is justified.

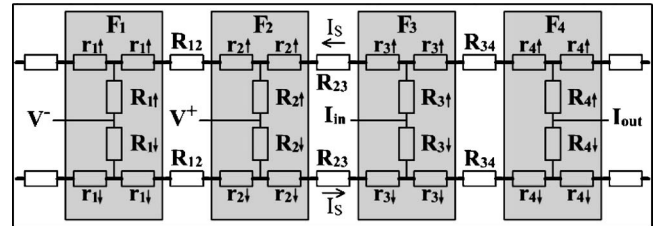


FIG. 4. A resistor model of our system (here, all four electrodes are assumed magnetized in the “up” direction). The upper half of the resistor network corresponds to the spin up ( $\uparrow$ ) transport channel in the nanotube. The lower half to the spin down ( $\downarrow$ ) channel. The resistance of the carbon nanotube between the cobalt contacts  $F_1$ – $F_2$ ,  $F_2$ – $F_3$ , and  $F_3$ – $F_4$  is equal to  $R_{12}/2$ ,  $R_{23}/2$ , and  $R_{34}/2$ , respectively. The contact between the carbon nanotube and ferromagnet  $F_i$  ( $i=1,2,3,4$ ) can be represented by a number of spin-dependent resistances  $R_{i,\eta}$  and  $r_{i,\eta}$  where  $\eta = \uparrow, \downarrow$  denotes spin. Assuming spin up to be the majority species, we have  $R_{i,\uparrow} < R_{i,\downarrow}$  and  $r_{i,\uparrow} < r_{i,\downarrow}$ . Due to the spin-dependent resistances in the current circuit ( $F_3$  and  $F_4$ ), the charge current  $I$  produces a finite spin current  $I_S$ . Due to the spin-dependent resistances in the voltage circuit ( $F_1$  and  $F_2$ ), a non-zero voltage difference  $V^+ - V^-$  consequently develops, leading to a finite nonlocal resistance  $R_{\text{nonloc}} \equiv (V^+ - V^-)/I$ .



Now, one can also calculate the expected “local” resistance change,<sup>30</sup> giving  $\Delta R_{\text{loc}} \approx 70 \Omega$  (for model B,  $170 \Omega$ , see Ref. 28). Consequently, only part of the magnetoresistance change in the conventional two-terminal geometry can be attributed to spin accumulation. Several mechanisms (AMR, Hall, TAMR-like effects) could be responsible for this difference. In particular, an important effect that has been ignored so far is the magnetocoulomb effect. This effect takes place in systems in the Coulomb blockade regime, weakly connected to ferromagnetic electrodes.<sup>17</sup> It can produce spin valvelike effects in the conventional two-terminal geometry. We estimate that resistance changes of several percents or more can occur [dependent on the strength of the Coulomb blockade and the charge state of the Coulomb island; for a detailed discussion, see (Ref. 18)].

Summarizing, we use a nonlocal measurement geometry to separate spin transport from charge transport in a single wall carbon nanotube contacted by ferromagnets. In this way, we unambiguously demonstrate spin accumulation in a carbon nanotube device. Not only does this work lead to a better understanding for future spin-based nanotube applications, it also opens the road to more sophisticated spin experiments on nanotubes (e.g., precession measurements and/or determination of the spin flip length  $\lambda_{sf}$  in carbon nanotubes).

We thank Bernard Wolfs, Siemon Bakker, Anthony England, Edgar Osorio, Marius Costache, Mihai Popinciuc, and Steve Watts for technical assistance and for useful discussions. This work was financed by MSC<sup>plus</sup> and NWO (via a “PIONIER” grant).

- 
- <sup>1</sup>R. H. Baughman, A. A. Zakhidov, and W. A. de Heer, *Science* **297**, 787 (2002).
- <sup>2</sup>K. Tsukagoshi, B. W. Alphenaar, and H. Ago, *Nature (London)* **401**, 572 (1999).
- <sup>3</sup>K. Tsukagoshi and B. W. Alphenaar, *Superlattices Microstruct.* **27**, 565 (2000).
- <sup>4</sup>J. R. Kim *et al.*, *Phys. Rev. B* **66**, 233401 (2002).
- <sup>5</sup>S. Chakraborty *et al.*, *Appl. Phys. Lett.* **83**, 1008 (2003).
- <sup>6</sup>D. Orgassa, G. J. Mankey, and H. Fujiwara, *Nanotechnology* **12**, 281 (2001).
- <sup>7</sup>B. Zhao *et al.*, *J. Appl. Phys.* **91**, 7026 (2002).
- <sup>8</sup>S. Sahoo, T. Kontos, C. Schönenberger, and C. Sürgers, *Appl. Phys. Lett.* **86**, 112109 (2005).
- <sup>9</sup>S. Sahoo, T. Kontos, J. Furer, C. Hoffmann, M. Gräber, A. Cottet, and C. Schönenberger, *Nat. Phys.* **1**, 99 (2005).
- <sup>10</sup>A. Jensen, Ph.D. thesis, Technical University of Denmark and University of Copenhagen, Copenhagen, Denmark, 2003.
- <sup>11</sup>A. Jensen, J. R. Hauptmann, J. Nygard, and P. E. Lindelof, *Phys. Rev. B* **72**, 035419 (2005).
- <sup>12</sup>B. Nagabhirava, T. Bansal, G. U. Suanasekera, B. W. Alphenaar, and L. Liu, *Appl. Phys. Lett.* **88**, 023503 (2006).
- <sup>13</sup>F. J. Jedema, A. T. Filip, and B. J. van Wees, *Nature (London)* **410**, 345 (2001).
- <sup>14</sup>B. W. Alphenaar, S. Chakraborty, and K. Tsukagoshi, in *Electron Transport in Quantum Dots* (Kluwer Academic/Plenum Publishers, New York, 2003), Chap. 11.
- <sup>15</sup>H. T. Man and A. F. Morpurgo, *Phys. Rev. Lett.* **95**, 026801 (2005).
- <sup>16</sup>C. Gould *et al.*, *Phys. Rev. Lett.* **93**, 117203 (2004).
- <sup>17</sup>K. Ono, H. Shimada, and Y. Ootuka, *J. Phys. Soc. Jpn.* **67**, 2852 (1998); H. Shimada, K. Ono, and Y. Ootuka, *J. Appl. Phys.* **93**, 8259 (2003).
- <sup>18</sup>S. J. van der Molen, N. Tombros, and B. J. van Wees, cond-mat/0604654, *Phys. Rev. B* (to be published June 2006).
- <sup>19</sup>M. Johnson and R. H. Silsbee, *Phys. Rev. Lett.* **55**, 1790 (1985).
- <sup>20</sup>F. J. Jedema *et al.*, *Nature (London)* **416**, 713 (2002).
- <sup>21</sup>SWNT’s from Nanostructured Amorphous Materials, Inc.
- <sup>22</sup>R. Krupke, F. Hennrich, H. v. Lhneysen, and M. M. Kappes, *Science* **301**, 344 (2003).
- <sup>23</sup>Although a yield of 1 out of 15 is low, it is comparable to the percentages obtained for two-terminal devices in Refs. 11 (4 out of 30) and 12 (1 out of 100).
- <sup>24</sup>This behavior was seen after a thermal cycling step and reproduced over eight consecutive curves. Similar effects can be deduced from Ref. 12, Fig. 4.
- <sup>25</sup>S. Krompiewski, *Phys. Status Solidi B* **2**, 226 (2005).
- <sup>26</sup>B. Bourlon *et al.*, *Phys. Rev. Lett.* **93**, 176806 (2004).
- <sup>27</sup>For Fig. 3(d) we obtain  $\alpha_F=0.29$ . The structure in this figure is attributed to the magnetization rotation as function of the external magnetic field. Probably, repeated thermal cycling changed the magnetic domain structure of the electrode.
- <sup>28</sup>For model B, we assume the nanotube below the ferromagnetic electrodes to be diffusive and in between the electrodes ballistic ( $R_{i,i+1}=0$ ). We extract a spin polarization  $\alpha_F=0.21$ . We calculate a value of  $170 \Omega$  for the local spin-valve geometry, a factor 4 smaller to the measured value.
- <sup>29</sup>From the resistor model we find that the influence of contacts  $F_1$  and  $F_4$  in the nonlocal measurement is very small [ $\sim 1 \Omega$  for Figs. 3(a)–3(c);  $\sim 3 \Omega$  for Fig. 3(d)].
- <sup>30</sup>F. J. Jedema, M. S. Nijboer, A. T. Filip, and B. J. van Wees, *Phys. Rev. B* **67**, 085319 (2003).
- <sup>31</sup>We independently checked that this does not provide an extra current path [see also A. Javey *et al.*, *Nature (London)* **424**, 654 (2003)].